Jyh-Ping Hsu[1]
Tien-Shiang Hsieh[1]
Tai-Horng Young[2]
Shiojenn Tseng[3]

[1]Department of Chemical Engineering, National Taiwan University, Taipei, Taiwan, R.O.C.
[2]Institute of Biomedical Engineering, College of Engineering, National Taiwan University, Taipei, Taiwan, R.O.C.
[3]Department of Mathematics, Tamkang University, Tamsui, Taipei, R.O.C.

Electrophoresis of biological cells: Charge-regulation and multivalent counterions association model

The electrophoresis of a biological cell is analyzed theoretically. An entity, which is of amphoteric nature, is used to simulate its electrophoretic behavior. To reflect conditions of practical interest, we assume that the liquid phase contains mixed (*a:b*)+(*c:b*) electrolytes, where *a* and *c* are the valences of cations, and *b* is the valence of anions. We consider the case where the surface of a cell contains both bivalent acidic and monovalent basic functional groups, the dissociation/association of them yields fixed surface charge, and the multivalent cations in the liquid phase are allowed to combine with dissociated acidic functional groups, which has the effect of lowering the charge density on cell surface. The electrophoretic behaviors of a cell under various conditions are illustrated. The results obtained can be used to identify the types of functional groups that may be present on cell surface. On the other hand, if the surface functional groups involved in cell electrophoresis are known, then their density and the associated dissociation/association constants can be estimated from experimental data.

Keywords: Amphoteric surface / Association of ionic species / Biological cells / Electrophoresis
EL 5364

1 Introduction

Entities with a linear size in the range from 10^{-5} to 10^{-9} m are called colloidal particles. Because the sizes of biological entities such as cells and microorganisms usually fall in this range, they are called biocolloids [1, 2]. Often, the surface properties of a biocolloid, especially its charged conditions, are characterized by electrophoresis [3–5]. Haydon and Seaman [4] concluded that the electrophoretic behavior of blood cells is mainly controlled by pH and ionic strength. The degree of dissociation the functional groups on cell surface is influenced by the former, and the thickness of double layer surrounding a cell is determined by the latter. These two factors are often examined in subsequent analyses [4]. Seaman *et al.* [5] pointed out that the attachment of Ca^{2+} on the surface of blood cell has the effect of lowering its surface potential. They found that, for fixed pH and ionic strength, increasing the concentration of Ca^{2+} in the liquid phase has the effect of decreasing cell mobility. The same phenomenon was observed by Mclaughlin *et al.* [6] for the case of lipid bilayer. Also, it was found that the addition of drugs in medium during incubation has the effect of reducing the number of functional groups on cell surface, which in turn, influences its electrophoretic mobility. Mironov and Dolgaya [7] investigated the electrophoretic behavior of rat neuron cells and found that it was influenced by pH, Ca^{2+} concentration, enzymes, and chemical modifying agents. They concluded that it is easier for Ca^{2+} to combine with neuron cells than divalent organic ions such as dimethonium. Since this has the effect of reducing the amount of negative charge on cell surface, the electrophoretic mobility of a cell decreases with the concentration of Ca^{2+}. Morita *et al.* [8] examined the electrophoretic behaviors of the lymphocyte subpopulations B cell and T cell of rat. They concluded that the density of the acidic and the basic functional groups in the cell membrane of these cells as well as the corresponding dissociation constants are different. Lytle *et al.* [9] discussed experimentally the effects of pH, ionic strength, and cations on the electrophoretic velocity of microorganisms.

For a rigid particle remained at constant surface potential, Smoluchowski showed that its electrophoretic velocity is proportional to the product of its surface potential and the applied electric field [1]. This model needs to be modified for the case of biological cells to take its nonrigid nature and specific surface conditions into account [10–25]. Various attempts, both experimental and theoretical, have been made in the past few decades [10–12]. Levine and Brooks [13] assumed that a red blood cell can be simu-

Correspondence: Dr. Jyh-Ping Hsu, Department of Chemical Engineering, National Taiwan University, Taipei, Taiwan 10617, R.O.C.
E-mail: jphsu@ccms.ntu.edu.tw
Fax: +886-2-23623040

 0173-0835/03/0905–1338 $17.50+.50/0

lated by a planar surface covered by an ion-penetrable membrane bearing fixed charge. They showed that for the case of low electrical potential the electrophoretic mobility obtained is smaller than that calculated by Smoluchowski's formula. The model of Levine and Brooks was modified by Ohshima and Kondo [14], and an approximate analytic expression for electrophoretic mobility was derived. The analysis was further extended by Hsu and Kuo [15] to the case of an asymmetric electrolyte. Tseng *et al.* [16] considered a charge regulation model and examined the effects of pH and ionic strength on the electrophoretic mobility of a biocolloid. Hsu and Chang [17] discussed the effect of the distribution of the functional groups in the membrane layer of a biocolloid on its electrophoretic behavior. The model of Levine and Brooks [13] was also adopted by Hsu *et al.* [15–17] and Ohshima *et al.* [10–12] to describe the electrophoresis of biocolloids. Hsu and Kuo [18] studied both particle-particle and particle-surface interactions by considering the case where the functional groups in the membrane layer of a particle carry multiple protons and the liquid phase contains mixed electrolytes. This model can be used to describe the adsorption of biocolloid to surface, the aggregation between two biocolloids, and the electrophoresis of colloids [19–21]. McLaughlin *et al.* [6] investigated the effect of adsorption of cations on the electrophoretic behavior of lipid bilayer. A similar analysis was conducted by Bentz [22], and Yamaguchi *et al.* [23] discussed the effect of the adsorption of Ca^{2+} to a lipid emulsion on its electrophoresis in a mixed electrolyte solution. Prieve and Ruckenstein [24] proposed a charge-regulated model to estimate the surface properties of red blood cells. In an analysis of the electrophoresis of a concentrated dispersion, Lee *et al.* [25] adopted a charge-regulated surface to simulate the behavior of biocolloids.

In the present study, the electrophoresis of a biological cell is investigated theoretically. In particular, the effects of the pH and the ionic strength of the liquid phase, the types of dissociation/association functional groups on cell surface and the associated dissociation/association constants, and the presence of the multivalent cations in the liquid phase on the electrophoretic behavior of a cell are discussed.

2 Theory

Because under conditions of practical significance the size of a cell is usually much larger than the thickness of double layer, the local curvature of the cell can be neglected. In this case, only a one-dimensional needed to be considered, that is, a cell can be viewed as a planar entity. Referring to Fig. 1, we consider a cell immersed in

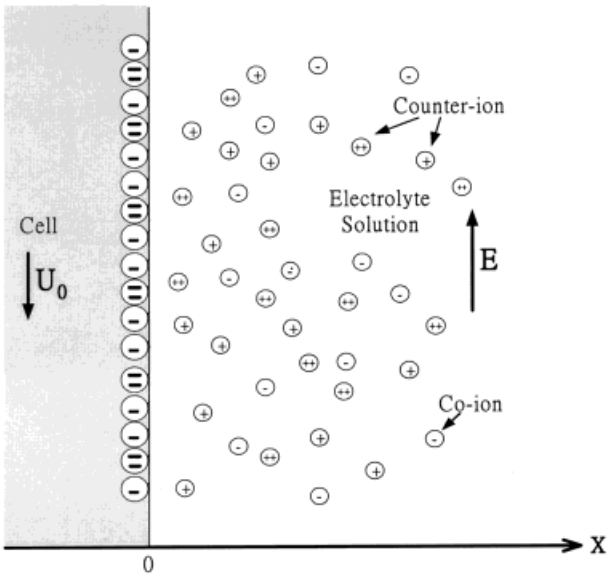

Figure 1. Schematic representation of the problem considered. An electric field *E* parallel to the surface of a cell is applied, U_0 is the electrophoretic velocity of the cell, and *X* is the scaled distance from cell surface.

a mixed (*a:b*)+(*c:b*) electrolyte solution; *a* and *c* are, respectively, the valences of monovalent and multivalent cations, and *b* is the valence of anions. An electric field *E* is applied in a direction parallel to cell surface, and the cell moves with velocity U_0. Suppose that the surface of a cell carries uniformly distributed acidic functional groups H_2A, basic functional groups B. Also, the divalent cation M^{2+} is allowed to bind to dissociated acidic functional groups. It can be shown that the scaled electrical potential φ can be described by the Poisson-Boltzmann equation (Addendum 5.1)

$$\frac{d^2\varphi}{dX^2} = \frac{\left[e^{b\varphi} - (1-\xi)e^{-a\varphi} - \xi e^{-c\varphi}\right]}{(a+b)+(c-a)\xi} \quad (1)$$

where the scaled variables are defined by $\varphi = F\phi/RT$, $\xi = cC_c^o/bC_b^o$, $\kappa^2 = F^2[a(a+b)C_a^o + c(b+c)C_c^o]/\varepsilon_0\varepsilon_r RT$, $X = \kappa r$. In these expressions, ϕ is the electrical potential, *F* is the Faraday constant, and *R* and *T* denote, respectively, the gas constant and the absolute temperature. The electroneutrality in the bulk liquid phase requires that $bC_b^o = aC_a^o + cC_c^o$, where ξ is the fraction of cations which has valence *c* in the bulk liquid phase, C_b^o, C_a^o, and C_c^o are, respectively the bulk concentrations of the ionic species of valences -*b*, *a*, and *c*, ε_r and ε_0 are respectively the relative permittivity of the liquid phase and the permittivity of a vacuum, κ and *r* are, respectively, the reciprocal Debye length, and the distance from cell surface. Here, φ and *X* are the scaled electric potential and the scaled distance from cell surface. The boundary conditions associated with Eq. (1) are assumed as

$$\frac{d\varphi}{dX} = \Gamma, \text{ as } X \to 0 \quad (2)$$

$$\frac{d\varphi}{dX} \to 0 \text{ and } \varphi \to 0 \text{ as } X \to \infty \quad (3)$$

The first condition arises from Gauss's law, where $\Gamma = \sigma F/\varepsilon_r\varepsilon_0 RT\kappa$ is the scaled surface charge density, σ being the surface charge density. The second condition implies that both the electrical potential and its derivative vanish at a point far away from cell surface.

Suppose that the functional groups H_2A and B on cell surface are capable of undergoing the following surface reactions:

$$H_2A \leftrightarrow H^+ + HA^- \quad (4)$$

$$HA^- \leftrightarrow H^+ + A^{2-} \quad (5)$$

$$HA^- + M^{2+} \leftrightarrow HAM^+ \quad (6)$$

$$A^{2-} + M^{2+} \leftrightarrow MA \quad (7)$$

$$BH^+ \leftrightarrow H^+ + B \quad (8)$$

Let K_{a1} and K_{a2} be the equilibrium dissociation constants of acidic functional groups, $K_{a1} = C_{H^+}C_{HA^-}/C_{H_2A}$, $K_{a2} = C_{H^+}C_{A^{2-}}/C_{HA^-}$, C_{HA^-}, $C_{A^{2-}}$, and C_{H^+} being, respectively, the surface concentration of HA^-, A^{2-}, and H^+, and K_b be the equilibrium dissociation constant of basic functional groups, $K_b = C_{H^+}C_B/C_{BH^+}$, C_{BH^+} and C_B being, respectively, the surface concentration of BH^+ and B. Suppose that the spatial variation of H^+ concentration follows Boltzmann distribution

$$C_{H^+} = C^0_{H^+}\exp(-\varphi) \quad (9)$$

where $C^0_{H^+}$ is the bulk concentration of H^+. For illustration, we assume that $c = 2$. Let K_{m1} and K_{m2} be the binding constants of the divalent cations M^{2+}, with $K_{m1} = C_{HAM^+}/(C_{HA^-}C_{M^{2+}})$, $K_{m2} = C_{MA}/(C_{A^{2-}}C_{M^{2+}})$, C_{HAM^+} and C_{MA} being, respectively, the surface concentration of HAM^+ and MA. Suppose that the spatial variation of the concentration of M^{2+} follow the Boltzmann distribution

$$C_{M^{2+}} = C^0_{M^{2+}}\exp(-2\varphi) \quad (10)$$

If we let N_{sa} and N_{sb} be the surface concentrations of acidic and basic dissociation functional groups, then

$$N_{sa} = C_{H_2A} + C_{HA^-} + C_{HAM^+} + C_{MA} \quad (11)$$

$$N_{sb} = C_{BH^+} + C_B \quad (12)$$

The surface charge density can be expressed as

$$\sigma F = (C_{BH^+} + C_{HAM^+} - C_{HA^-} - 2C_{A^{2-}}) \quad (13)$$

It can be shown that (Addendum 5.2)

$$\sigma = FN_{sb}\left[\frac{C_{H^+}}{C_{H^+} + K_b}\right] + \quad (13a)$$

$$+ FN_{sa}\left[\frac{C_{H^+}K_{a1}K_{m1}C_{M^{2+}} - C_{H^+}K_{a1} - 2K_{a1}K_{a2}}{C^2_{H^+} + C_{H^+}K_{a1}K_{a2} + C_{H^+}K_{a1}K_{m1}C_{M^{2+}} + K_{a1}K_{a2}K_{m2}C_{M^{2+}}}\right]$$

Suppose that the flow field can be described by the Navier-Stokes equation [26]

$$\frac{d^2U}{dX^2} = L\frac{e^{b\varphi} - (1-\xi)e^{-a\varphi} - \xi e^{-c\varphi}}{(a+b) + (c-a)\xi} \quad (14)$$

where the scaled variables are defined by $U = u/U_0$ and $L = \varepsilon_0\varepsilon_r RTE/\eta FU_0$, u and U_0 being, respectively, the velocities of the liquid phase near and far away from the particle, and U and E being, respectively, the magnitude of the scaled velocity and the strength of the applied electric field; η is the viscosity of the liquid phase. For convenience, the cell is held fixed at steady state, and the liquid moves in the inverse direction as that of U_0. Therefore, the boundary conditions associated with Eq. (14) are

$$U = 0 \text{ as } X \to 0 \quad (15)$$

$$U \to -1 \text{ as } X \to \infty \quad (16)$$

The electric field and the flow field are determined by solving Eqs. (1) and (14) simultaneously subject to boundary conditions, Eqs. (2), (3), (15), and (16), and the results obtained can be used to calculate the electrophoretic mobility of a cell, $\mu = U_0/E$.

3 Results and discussion

The governing equations are solved by a finite difference method based on central difference [27]. For illustration, we consider the case $a = 1$, $b = 1$, $c = 2$, $T = 298$ K, $\varepsilon_r = 78.5$, and $E = 1000$ V/m. The level of ionic strength assumed is based on the experimental work of Mironov and Dolgaya [7]. The surface potential can be evaluated based on an iterative procedure (Addendum 5.3). Also, in the numerical simulations presented below, some of the dissociation/association constants are inferred from Mironov and Dolgaya [7], and we assume others. Similarly, the values of N_{sa} and N_{sb} are inferred from our previous results for cerelellar granule neurons [29].

Figure 2 illustrates the variation of cell mobility μ as a function of pH under various conditions. Curves 1, 3, and 5 are the results based on the present model, and curves 2 and 4 are those based on a monovalent acidic functional groups without basic functional groups. For the case of curves 2 and 4, $|\mu|$ increases with the increase in pH, and it vanishes if pH is sufficiently low. This is because in curves 2 and 4, cell surface contains monovalent

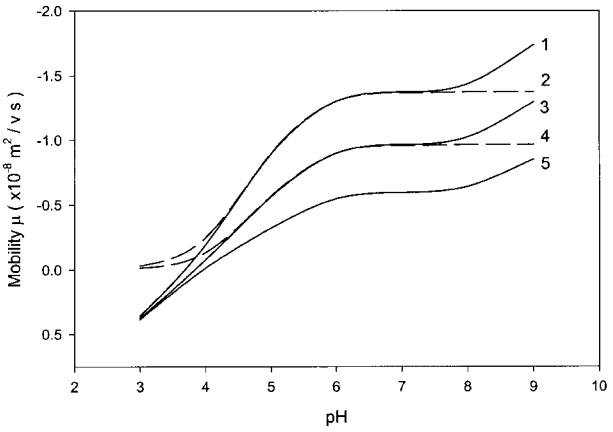

Figure 2. Variation of cell mobility μ as a function of pH for the case of ionic strength = 8.5 mM and ξ = 0.615. Curve 1, $N_{sa} = 1.0 \times 10^{-7}$ mol/m^2; 3, $N_{sa} = 5.0 \times 10^{-8}$ mol/m^2; 5, $N_{sa} = 2.5 \times 10^{-8}$ mol/m^2. Parameters used are $N_{sb} = 5.0 \times 10^{-8}$ mol/m^2, $K_{a1} = 1.0 \times 10^{-5}$ M, $K_{a2} = 1.0 \times 10^{-9}$ M, $K_{m1} = 50$ M^{-1}, $K_{m2} = 0$ M^{-1}, $K_b = 3.0 \times 10^{-3}$ M. Curve 2, $N_{sa} = 1.0 \times 10^{-7}$ mol/m^2; 4, $N_{sa} = 5.0 \times 10^{-8}$ mol/m^2. Parameters used: $N_{sb} = 0$ mol/m^2, $K_{a1} = 1.0 \times 10^{-5}$ M, $K_{a2} = 0$ M, $K_{m1} = 50$ M^{-1}, $K_{m2} = 0$ M^{-1}, $K_b = 0$ M.

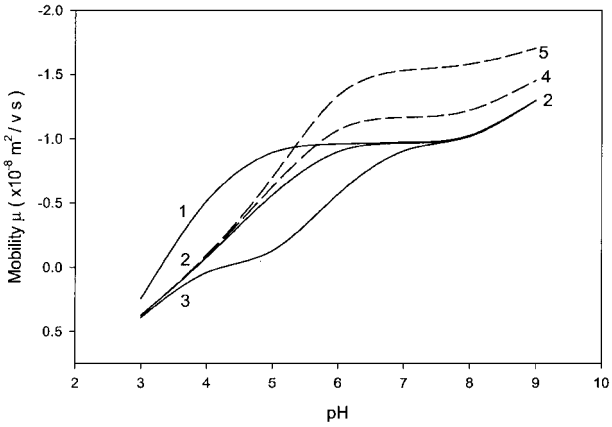

Figure 3. Variation of cell mobility μ as a function of pH for the case of ionic strength = 8.5 mM, ξ = 0.615, $N_{sa} = 5.0 \times 10^{-8}$ mol/m^2, $N_{sb} = 5.0 \times 10^{-8}$ mol/m^2, $K_{a2} = 1.0 \times 10^{-9}$ M, $K_b = 3.0 \times 10^{-3}$ M, and $K_{m2} = 0$ M^{-1}. Curve 1, $K_{a1} = 1.0 \times 10^{-4}$ M, 2; $K_{a1} = 1.0 \times 10^{-5}$ M; 3, $K_{a1} = 1.0 \times 10^{-6}$ M. $K_{m1} = 50$ M^{-1} in these curves. Curve 4, $K_{m1} = 25$ M^{-1}; 5, $K_{m1} = 0$ M^{-1}. $K_{a1} = 1.0 \times 10^{-5}$ M in these curves.

acidic functional groups only. The dissociation of these functional groups leads to a negatively charged surface, and the higher the pH, the more complete the degree of dissociation. If pH is sufficiently low, cell surface becomes essentially uncharged. For the case of curves 1, 3, and 5, if μ is negative, $|\mu|$ increases with the increase in pH, and if μ is positive, $|\mu|$ increases with the decrease in pH. This is because in curves 1, 3, and 5, cell surface contains both acidic and basic functional groups. If pH is low, cell surface becomes positively charged, and the lower the pH the higher the charge density on cell surface. Figure 2 also shows that if pH exceeds about 7, curves 1, 3, and 5 have an inflection point at about pH 7, which is not observed for the case of curves 2 and 4. Apparently, the inflection point arises from the dissociation of the second H^+ in the acidic functional group of the present model. The experimental results of Haydon and Seaman [4] for blood cells showed that μ is constant if pH exceeded pH 7, which implies that the surface property of blood cells is governed by mono-valent acidic functional groups. On the other hand, the electrophoretic results of Mironov and Dolgaya [7] for isolated rat dorsal root ganglion neurons revealed that μ keeps on increasing even if pH is higher than 7, suggesting the presence of multivalent acidic functional groups. Similar behavior was also observed by Lytle *et al.* [9] for the case of microorganism.

The effect of dissociation constant K_{a1} and association constant K_{m1} on cell mobility μ is examined in Fig. 3 where its variation as a function of pH is plotted. Curves 1–3 of this figure suggest that for a fixed pH, if μ is negative, the larger the K_{a1}, the greater the $|\mu|$, which is expected, since the larger K_{a1} the more complete the dissociation of the first H^+ of an acidic functional group on cell surface. Note that if pH is sufficiently high, because the surface charge of a cell is dominated by K_{a2}, all three curves lead to the same μ. The effect of the association of Ca^{2+} with dissociated acidic functional groups can be seen in curves 2, 4, and 5. Here, the larger the K_{m1}, the smaller the $|\mu|$ if μ is negative, and the reverse is true if μ is positive. This is because the larger the K_{m1}, the more significant the association of Ca^{2+} with dissociated acidic functional group, therefore, the smaller the charge density on cell surface. Note that if pH is sufficiently low curves 2, 4, and 5 degenerate to the same value. This is because if pH is low, the dissociation of acidic functional groups becomes negligible. The association of Ca^{2+} to cell surface was observed by Seaman *et al.* [5] and Mclaughlin *et al.* [6]. Mironov and Dolgaya [7] pointed out that for the case of neuron cells the increase of Ca^{2+} in the liquid phase increases its shielding ability and its association to cell surface. Both of these effects yield a smaller mobility.

The effects of K_{a2} and N_b on cell mobility is illustrated in Fig. 4 where μ is plotted as a function of pH. Curves 1, 3, and 5 of this figure reveal that the larger K_{a2}, the larger the $|\mu|$. This is expected because a larger K_{a2} leads to a higher negative charge density on cell surface. Note that because $K_{a2} = 0$ in curve 3 of Fig. 4 μ behaves the same as that for the case of monovalent acidic functional groups

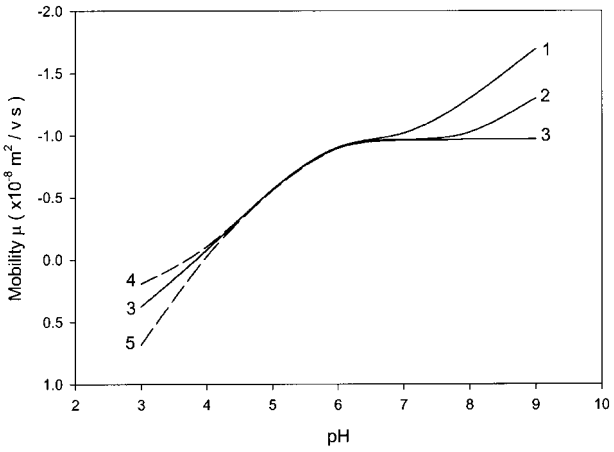

Figure 4. Variation of cell mobility μ as a function of pH for the case of ionic strength = 8.5 mM, $\xi = 0.615$, $N_{sa} = 5.0 \times 10^{-8}$ mol/m^2, $K_{m1} = 50$ M^{-1}, $K_{m2} = 0$ M^{-1}, $K_b = 1.0 \times 10^{-12}$ M. Curve 1, $K_{a2} = 1.0 \times 10^{-8}$ M; 2, $K_{a2} = 1.0 \times 10^{-9}$ M; 3, $K_{a2} = 0$ M. $K_{a1} = 1.0 \times 10^{-5}$ M and $N_{sb} = 5.0 \times 10^{-8}$ mol/m^2 in these curves. Curve 4, $N_{sb} = 2.5 \times 10^{-8}$ mol/m^2; 5, $N_{sb} = 1.0 \times 10^{-7}$ mol/m^2. $K_{a2} = 0$ M in these curves.

(curve 2 or 4 in Fig. 2) when pH is high. However, due to the presence of basic functional groups (*i.e.*, $N_{sb}\ \mu \neq 0$) μ does not approach zero when pH is low. Curves 4 and 5 of Fig. 4 suggest that for a fixed K_{a2}, $|\mu|$ increases with the increase in N_{sb} if pH is low, and it is almost independent of N_{sb} if pH is high. This is because the larger the N_{sb} the higher the positive surface charge density, and therefore, for a fixed pH, the lower the negative surface charge density. In general, an increase in either K_{a1} or K_{a2}, leads to a greater negative mobility, and an increase in N_{sb} leads to a greater positive mobility.

The variations of cell mobility μ as a function of ionic strength at various pH and ξ are presented in Fig. 5. As can be seen in this figure if pH is high, the surface of a cell is positively charged, and the higher the pH, the higher the surface charge density, and therefore, the larger the $|\mu|$. On the other hand, if pH is low, the surface of a cell becomes positively charged. In both cases $|\mu|$ decreases with an increase in ionic strength, and approaches to the same constant value. This is because the higher the ionic strength, the thinner the double layer surrounding a cell, and the stronger the shielding effect of counterions. The qualitative behaviors of the electrophoretic data reported by Morita *et al.* [8] are consistent with that predicted by curve 4 of Fig. 5a. That is, at low pH and low ionic strength μ is positive, and as ionic strength is increased at a fixed pH, μ approaches zero. The effect of the types of electrolyte on the electrophoretic behavior of a cell is illustrated in Fig. 5b. Here, curves 1 and 3 represent, respectively, the case where the liquid phase contains only 1:1 and 2:1 electrolyte, and the liquid phase contains a mixed 1:1 and 2:1 electrolytes for the case of curve 2. Figure 5b indicates that for the same pH and ionic strength, the greater the fraction of divalent cations in the liquid phase, the smaller the $|\mu|$. This is because divalent cations are capable of combining with dissociated acidic functional groups on cell surface, which has the effect of reducing the charge density. Figure 5b also indicates that $|\mu|$ may decrease with the increase in κa even when divalent cations are absent. This behavior is different from that for the case when particle surface is remained at a constant potential, and is typical to the present charge-regulated surface [8, 10]. The decrease in $|\mu|$ as κa increases can be explained by that the space available for the distribution of dissociated ionic species

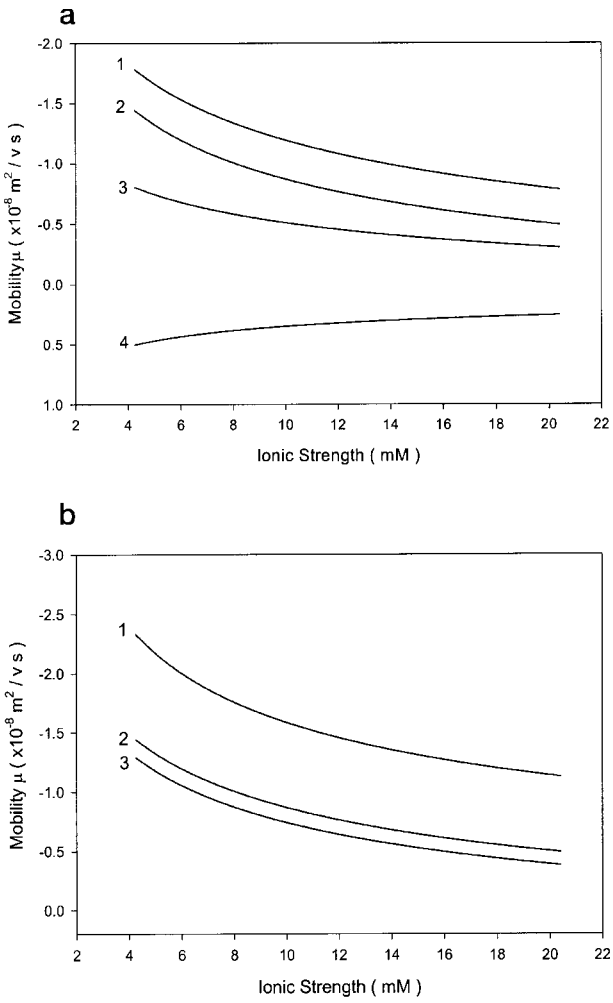

Figure 5. Variation of cell mobility μ as a function of ionic strength for the case of $N_{sa} = 5.0 \times 10^{-8}$ mol/m^2, $N_{sb} = 5.0 \times 10^{-8}$ mol/m^2, $K_{a1} = 1.0 \times 10^{-5}$ M, $K_{a2} = 1.0 \times 10^{-9}$ M, $K_{m1} = 50$ M^{-1}, $K_{m2} = 0$ M^{-1}, $K_b = 3.0 \times 10^{-12}$ M. (a) $\xi = 0.615$, curve 1, pH 9; 2, pH 7; 3, pH 5; 4, pH 3. (b) pH 7, curve 1, $\xi = 0$; 2, $\xi = 0.615$; 3, $\xi = 1$.

becomes small as double layer is thin, and therefore, the degree of dissociation of the functional groups on particle surface is low [28].

Figure 6 shows the variation of cell mobility μ as a function of the concentration of M^{2+} at various K_{m1}. The ionic strength is fixed in Fig. 6b. The ionic strength in Fig. 6a for the case the concentration of M^{2+} is lower than 2.0 mM is lower than that in Fig. 6b, and therefore, $|\mu|$ of the former is larger than $|\mu|$ of the latter. As can be seen in Fig. 6, $|\mu|$ decreases with the increase in K_{m1} which is expected because the larger the K_{m1} the more significant the combination of M^{2+} with dissociated acidic functional groups. Figure 6a reveals that $|\mu|$ decreases with the increase in the concentration of M^{2+}. The decrease in $|\mu|$ is the result of two factors: the shielding effect due to the increase in ionic strength, and the combination of M^{2+} with dissociated acidic functional groups. Figure 6b indicates that, for a fixed ionic strength, $|\mu|$ decreases with the increase in the concentration of M^{2+}. This is consistent with the results shown in Fig. 5b. The qualitative behavior of the curves shown in Fig. 6b is consistent with the experimental observation of Seaman *et al.* [5], for red blood cells, that is, if ionic strength is fixed, the mobility of a cell decreases with the increase in Ca^{2+} concentration.

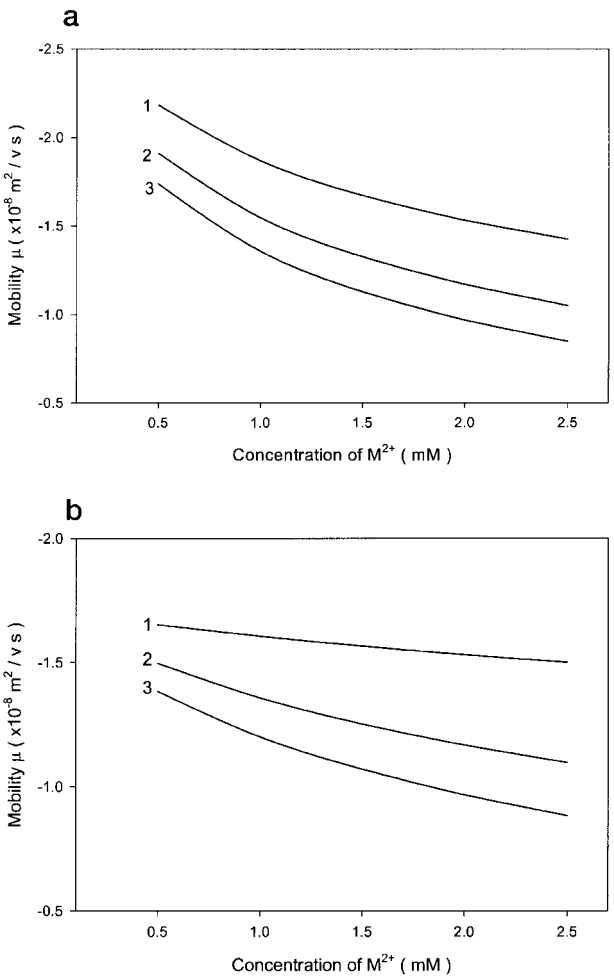

Figure 6. Variation of cell mobility μ as a function of M^{2+} concentration at various K_{m1} for the case of $N_{sa} = 5.0\times10^{-8}$ mol/m^2, $N_{sb} = 5.0\times10^{-8}$ mol/m^2, $K_{a1} = 1.0\times10^{-5}$ M, $K_{a2} = 1.0\times10^{-9}$ M, $K_{m2} = 0$ M^{-1}, $K_b = 3.0\times10^{-3}$ M, pH 7. (a) Curve 1, $K_{m1} = 0$ M^{-1}; 2, $K_{m1} = 25$ M^{-1}; 3, $K_{m1} = 50$ M^{-1}. (b) Ionic strength = 8.5 mM, curve 1, $K_{m1} = 0$ M^{-1}; 2, $K_{m1} = 25$ M^{-1}; 3, $K_{m1} = 50$ M^{-1}.

It should be pointed out that the specific behavior of cell mobility at high pH, such as that of curve 1 of Fig. 2, might also arise from other mechanism. For instance, there may have several types of monovalent acidic functional group on cell surface with different equilibrium dissociation constants [24]. Figure 7 shows the simulated variation in the mobility of a cell as a function of pH for the case when cell surface contains two types of acidic functional group and one type of basic functional group. Here, the association of multivalent cations with dissociated functional groups is neglected. The derivation of surface charge density is presented in Addendum 5.4. Note that the qualitative behavior of the curve in Fig. 7 is similar to that of Fig. 2 for the case when the cell surface contains both divalent acidic functional groups and basic functional groups.

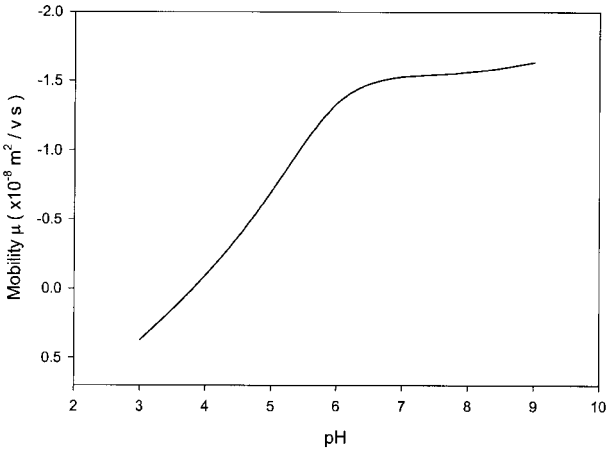

Figure 7. Simulated variation of cell mobility μ as a function of pH for the case cell surface contains two types of monovalent acidic functional group and one type of basic functional group. Parameters used are ionic strength = 8.5 mM, $\xi = 0.615$. $N_{sa1} = 5.0\times10^{-8}$ mol/m^2, $N_{sa2} = 5.0\times10^{-8}$ mol/m^2, $N_{sb} = 5.0\times10^{-8}$ mol/m^2, $K_{sa1} = 1.0\times10^{-5}$ M, $K_{sa2} = 1.0\times10^{-9}$ M, $K_b = 3.0\times10^{-3}$ M.

This work is supported by the National Science Council of the Republic of China.

Received September 24, 2002

4 References

[1] Hunter, R. J., *Foundations of Colloid Science*, Oxford University Press, Oxford, UK 1989, Vol. 1.

[2] Shaw, D. J., *Introduction to Colloid and Surface Chemistry*, 4th ed., Butterworth-Heinemann, Oxford, UK 1993.

[3] Seaman, G. V. F., Heard, D. H., *Blood* 1961, 18, 599–604.

[4] Haydon, D. A., Seaman, G. V. F., *Arch. Biochem. Biophys.* 1967, *122*, 126–136.

[5] Seaman, G. V. F., Vassar, P. S., Kendal, M. J., *Arch. Biochem. Biophys.* 1969, *135*, 356–362.

[6] McLaughlin, S., Mulrine, N., Gresalfi, T., Vio, G., McLaughlin, A. J., *Gen. Physiol. Rev.* 1981, *77*, 445–473.

[7] Mironov, S. L., Dolgaya, E. V., *J. Membrane Biol.* 1985, *86*, 197–202.

[8] Morita, K., Muramatsu, N., Ohshima, H., Kondo, T., *J. Colloid Interface Sci.* 1991, *147*, 457–461.

[9] Lytle, D. A., Johnson, C. H., Rice E. W., *Colloids Surfaces B* 2002, *24*, 91–101.

[10] Kawahata, S., Ohshima, E. V., Muramatsu, N., Kondo, T., *J. Colloid Interface Sci.* 1990, *138*, 182–282.

[11] Makino, K., Ikekita, M., Kondo, T., Tanuma, S., Ohshima, H., *Colloid Polym. Sci.* 1994, *272*, 487–492.

[12] Makino, K., Fukai, F., Kawaguchi, T., Ohshima, H., *Colloids Surfaces B* 1995, *5*, 221–226.

[13] Levine, S., Levine, M., Sharp, K. A., Brooks, D. E., *Biophys. J.* 1983, *42*, 127–135.

[14] Ohshima, H., Kondo, T., *J. Colloid Interface Sci.* 1987, *116*, 305–311.

[15] Hsu, J. P., Kuo, Y. C., *J. Colloid Interface Sci.* 1994, *166*, 208–214.

[16] Tseng, S., Lin, S. H., Hsu, J. P., *Colloids Surfaces B* 1999, *13*, 277–286.

[17] Hsu, J. P., Hsu, W. C., Chang, Y. I., *Colloid Polym. Sci.* 1994, *272*, 251–260.

[18] Hsu, J. P., Kuo, Y. C., *J. Colloid Interface Sci.* 1996, 183, 194–198.

[19] Hsu, J. P., Kuo, Y. C., *Langmuir* 1997, *13*, 4372–4376.

[20] Huang, S. W., Hsu, J. P., Kuo, Y. C., Tseng, S., *J. Phys. Chem. B* 2002, *106*, 2117–2122.

[21] Hsu, J. P., Huang, S. W., Kuo, Y. C., Tseng, S., *J. Phys. Chem. B* 2002, *106*, 4269–4275.

[22] Bentz, J., *J. Colloid Interface Sci.* 1982, *90*, 164–182.

[23] Yamaguchi, T., Nishizaki, K., Itai, S., Nemoto, M., Ohshima, H., *Colloids Surfaces B* 1995, *5*, 49–55.

[24] Prieve, D. C., Ruckenstein E., *J. Theor. Biol.* 1976, *56*, 205–228.

[25] Lee, E., Yen, F. Y., Hsu, J. P., *Electrophoresis* 2000, *21*, 475–480.

[26] Bird, R. B., Stewart, W. E., Ligthtfoot, E. N., *Transport Phenomena*, Oxford University Press, New York 1960.

[27] Davis, M. E., *Numerical Methods and Modeling for Chemical Engineers*, John Wiley & Sons, New York 1984.

[28] Tang, Y. P., Chih, M. H., Lee, E., Hsu, J. P., *J. Colloid Interface Sci.* 2001, *242*, 121–126.

[29] Hsu, J. P., Huang, S. W., Hsieh, T. S., Young, T. H., Hu, W. W., *Electrophoresis* 2002, *23*, 2001–2006.

5 Addendum

5.1

The liquid phase contains mixed (*a:b*)+(*c:b*) electrolytes. Assuming Boltzmann distribution for each ionic species, the Poisson equation becomes

$$\frac{d^2\phi}{dr^2} = \frac{1}{\varepsilon_r\varepsilon_0}\left[bC_b^0 F\exp\left(\frac{bF\phi}{RT}\right) - aC_a^0 F\exp\left(\frac{-aF\phi}{RT}\right) - cC_c^0 F\exp\left(\frac{-cF\phi}{RT}\right)\right] \quad \text{(A-1)}$$

The electroneutrality in the liquid phase requires that $bC_b^0 = aC_a^0 + cC_c^0$. Because $\varphi = F\phi/RT$, $\xi = cC_c^0/bC_b^0$, Eq. (A-1) becomes

$$\frac{d^2\phi}{dr^2} = \frac{bC_b^0 F}{\varepsilon_r\varepsilon_0}\left[e^{b\varphi} - (1-\xi)e^{-a\varphi} - \xi e^{-c\varphi}\right] \quad \text{(A-2)}$$

Because $X = \kappa r$, $\kappa = (2F^2I/\varepsilon_r\varepsilon_0 RT)^{1/2}$, and $I = (a^2C_a^0 + b^2C_b^0 + c^2C_c^0)/2 = [a(a+b)C_a^0 + c(b+c)C_c^0]/2$, Eq. (A-2) becomes

$$\frac{d^2\varphi}{dX^2} = \frac{bC_b^0 F^2}{\kappa^2\varepsilon_r\varepsilon_0 RT}\left[e^{b\varphi} - (1-\xi)e^{-a\varphi} - \xi e^{-c\varphi}\right] =$$

$$= \frac{bC_b^0}{\left[a(a+b)C_a^0 + c(c+b)C_c^0\right]}\left[e^{b\varphi} - (1-\xi)e^{-a\varphi} - \xi e^{-c\varphi}\right] =$$

$$= \frac{\left[e^{b\varphi} - (1-\xi)e^{-a\varphi} - \xi e^{-c\varphi}\right]}{(a+b) + (c-a)\xi} \quad \text{(A-3)}$$

5.2

From Eqs. (4)–(8) we have

$$C_{HA^-} = \frac{C_{H_2A}K_{a1}}{C_{H^+}} \quad \text{(B-1)}$$

$$C_{A^{2-}} = \frac{C_{H_2A}K_{a1}K_{a2}}{C_{H^+}^2} \quad \text{(B-2)}$$

$$C_{HAM^+} = \frac{C_{H_2A}C_{M^{2+}}K_{a1}K_{m1}}{C_{H^+}} \quad \text{(B-3)}$$

$$C_{MA} = \frac{C_{H_2A}C_{M^{2+}}K_{a1}K_{a2}K_{m2}}{C_{H^+}^2} \quad \text{(B-4)}$$

Substituting these expressions into Eq. (11) yields

$$C_{HA^-} = \frac{C_{H^+}K_{a1}N_{sa}}{C_{H^+}^2 + C_{H^+}K_{a1} + K_{a1}K_{a2} + C_{H^+}K_{a1}K_{m1}C_{M^{2+}} + K_{a1}K_{a2}K_{m2}C_{M^{2+}}} \tag{B-5}$$

$$C_{A^{2-}} = \frac{K_{a1}K_{a2}K_{sa}}{C_{H^+}^2 + C_{H^+}K_{a1} + K_{a1}K_{a2} + C_{H^+}K_{a1}K_{m1}C_{M^{2+}} + K_{a1}K_{a2}K_{m2}C_{M^{2+}}} \tag{B-6}$$

The surface concentrations of positively charged species are

$$C_{HAM^+} = \frac{C_{H^+}K_{a1}K_{m1}C_{M^{2+}}N_{sa}}{C_{H^+}^2 + C_{H^+}K_{a1} + K_{a1}K_{a2} + C_{H^+}K_{a1}K_{m1}C_{M^{2+}} + K_{a1}K_{a2}K_{m2}C_{M^{2+}}} \tag{B-7}$$

$$C_{BH^+} = N_{sb}\frac{C_{H^+}}{C_{H^+}K_b} \tag{B-8}$$

Substituting these expressions into Eq. (13) leads to Eq. (13a) in the text.

For the case the surface of a cell carriers only acidic functional groups, N_{sb}, K_{m1}, and K_{m2} all vanish, and Eq. (13a) becomes

$$\sigma = -FN_{sa}\left[\frac{C_{H^+}K_{a1} + 2K_{a1}K_{a2}}{C_{H^+}^2 + C_{H^+}K_{a1} + K_{a1}K_{a2}}\right] \tag{B-9}$$

5.3

Equation (1) can be rewritten as

$$\frac{d}{dX}\left(\frac{d\varphi}{dX}\right)^2 = \left[\frac{2}{(a+b)+(c-a)\xi}\right]\frac{d}{dX}\left(\frac{1}{b}e^{b\varphi} + \left(\frac{1-\xi}{a}\right)e^{-a\varphi} + \frac{\xi}{c}e^{-c\varphi} + D\right) \tag{C-1}$$

where D is a constant. Integrating this expression with respect to X gives

$$\int_0^{(d\varphi/dX)^2} d[(d\varphi/dX)]^2 =$$

$$= \left[\frac{2}{(a+b)+(c-a)\xi}\right]\int_{\frac{1}{b}+\frac{1}{a}+\left(\frac{1}{c}-\frac{1}{a}\right)\xi+D}^{\frac{1}{b}e^{b\varphi}+\left(\frac{1-\xi}{a}\right)e^{-a\varphi}+\frac{\xi}{c}e^{-c\varphi}+D} d\left(\frac{1}{b}e^{b\varphi} + \left(\frac{1-\xi}{a}\right)e^{-a\varphi} + \frac{\xi}{c}e^{-c\varphi} + D\right) \tag{C-2}$$

Letting $X = 0$ in this expression gives

$$\frac{d\varphi}{dX}\Big|_{\varphi_0} = \left[\frac{2}{(a+b)+(c-a)\xi}\right]^{1/2}\left[\frac{1}{b}e^{b\varphi_0} + \left(\frac{1-\xi}{a}\right)e^{-a\varphi_0} + \frac{\xi}{c}e^{-c\varphi_0} - \frac{1}{b} - \frac{1}{a} - \left(\frac{1}{c}-\frac{1}{a}\right)\xi\right]^{1/2} \tag{C-3}$$

For the case $a = 1$, $b = 1$, $c = 2$, we have

$$\frac{d\varphi}{dX} = \left[\frac{2}{2+\xi}\right]^{1/2}\left[e^{\varphi_0} + (1-\xi)e^{-\psi_0} + \frac{\xi}{2}e^{-2\varphi_0} - \left(2 - \frac{\xi}{2}\right)\right]^{1/2} \tag{C-4}$$

$$\frac{d\varphi}{dX} = \left[\frac{2}{2+\xi}\right]^{1/2}(e^{-\varphi_0} - 1)\left[e^{\varphi_0} + \frac{\xi}{2}\right]^{1/2} \tag{C-5}$$

Combining Eqs. (2) and (C-5), and considering the case that N_{sb}, K_{m1}, and K_{m2} all vanish, we obtain

$$\left[\frac{2}{2+\xi}\right]^{1/2}(e^{-\varphi_0} - 1)\left[e^{\varphi_0} + \frac{\xi}{2}\right]^{1/2} = \frac{F^2N_{sa}}{\varepsilon_r\varepsilon_0RT\kappa}\left[\frac{K_{a1}C_{H^+}^0e^{-\varphi_0} + 2K_{a1}K_2}{C_{H^+}^{0\,2}e^{-2\varphi_0} + K_{a1}C_{H^+}^0e^{-\varphi_0} + K_{a1}K_{a2}}\right] \tag{C-6}$$

This equation can be solved iteratively to obtain the surface potential.

5.4

Consider the case where cell surface contains two types of monovalent acidic functional groups, HA_1, and HA_2, and one type of basic functional groups, BH. The dissociation reactions of these functional groups can be expressed as

$$HA_1 \leftrightarrow H^+ + A_1^- \quad \text{(D-1)}$$

$$HA_2 \leftrightarrow H^+ + A_2^- \quad \text{(D-2)}$$

$$BH^+ \leftrightarrow H^+ + B \quad \text{(D-3)}$$

Let K_{sa1} and K_{sa2} be the equilibrium dissociation constants of acidic functional groups HA_1 and HA_2, respectively, $K_{sa1} = C_{H^+}C_{A_1^-}/C_{HA_1}$, $K_{sa2} = C_{H^+}C_{A_2^-}/C_{HA_2}$, and K_b be the equilibrium dissociation constant of basic functional groups, $K_b = C_{H^+}C_B/C_{BH^+}$. Suppose that the spatial variation of H^+ concentration follows Boltzmann distribution.

If we let N_{sa1}, N_{sa2}, and N_{sb} be the surface concentrations of functional groups, HA_1, HA_2, and BH^+, respectively, then

$$N_{sa1} = C_{HA_1} + C_{A_1^-} \quad \text{(D-4)}$$

$$N_{sa2} = C_{HA_2} + C_{A_2^-} \quad \text{(D-5)}$$

$$N_{sb} = C_{BH^+} + C_B \quad \text{(D-6)}$$

The surface charge density can be expressed as

$$\sigma = F(C_{BH^+} - C_{A_1^-} - C_{A_2^-}) \quad \text{(D-7)}$$

Therefore,

$$\sigma = F\left[\frac{N_{sb}}{1 + \frac{K_b}{C_{H^+}}}\right] - F\left[\frac{N_{sa1}}{1 + \frac{C_{H^+}}{K_{sa1}}} + \frac{N_{sa2}}{1 + \frac{C_{H^+}}{K_{sa2}}}\right] \quad \text{(D-8)}$$